INSTITUTE OF PHYSICS PUBLISHING INVERSE PROBLEMS

Inverse Problems **23** (2007) 373–383 doi:10.1088/0266-5611/23/1/021

Explicit inversion formulae for the spherical mean Radon transform

Leonid A Kunyansky

Department of Mathematics, University of Arizona, Tucson, AZ 85721, USA

E-mail: leonk@math.arizona.edu

Received 20 October 2006, in final form 25 October 2006
Published 17 January 2007
Online at stacks.iop.org/IP/23/373

Abstract

We derive explicit formulae for the reconstruction of a function from its integrals over a family of spheres, or for the inversion of the spherical mean Radon transform. Such formulae are important for problems of thermo- and photo-acoustic tomography. A closed-form inversion formula of a filtration-backprojection type is found for the case when the centres of the integration spheres lie on a sphere in $\mathbb{R}^n$ surrounding the support of the unknown function.

Introduction

The problem of the reconstruction of a function from its spherical integrals (or means) has recently attracted the attention of researchers due to its connection to the thermo-acoustic and photo-acoustic tomography [12, 13, 21, 22]. In these imaging modalities, the object of interest is illuminated by a short electromagnetic pulse which causes a fast expansion of the tissue. The intensity of the resulting ultrasound wave is recorded by a set of detectors surrounding the object. The local intensity of such expansion is of significant medical interest: it depends on the physical properties of the tissue (such as, for example, water content) and its anomaly can be indicative of tumours. Under certain simplifying assumptions the measurements can be represented by the integrals of the expansion intensity over the spheres with the centres at the detectors' locations. The reconstruction of the local properties from these integrals is equivalent to the inversion of the spherical mean Radon transform.

An introduction to the subject can be found in [12–14]; for the important results on the injectivity of the spherical Radon transform and the corresponding range conditions we refer the reader to [2–4, 9, 10]. In the present paper we concentrate on explicit inversion formulae which are important from both theoretical and practical points of view. Most of the known formulae of this sort pertain to the spherical acquisition geometry, i.e. to the situation when centres of the integration spheres (the positions of the detectors) lie on a sphere surrounding the body. Such are the series solutions for 2D and 3D presented in [15, 16, 21]. More desirable backprojection-type formulae were derived in [9] for odd-dimensional spaces, and

implemented in [6]. A different explicit formula for the spherical acquisition geometry valid in 3D was found in [22] (together with formulae for certain unbounded acquisition surfaces).

In this paper we present a set of explicit closed-form inversion formulae of the filtration/backprojection type for the spherical geometry in $\mathbb{R}^n$, $n \geqslant 2$. Such formulae for the even-dimensional cases were not known previously; a set of different inversion formulae in even dimensions was announced by Finch [11] during the tomography meeting in Oberwolfach in August 2006, where our results were also presented for the first time.

We discuss the theoretical foundations of our method in sections 1 to 3, and present the results of numerical implementation in section 4.

1. Formulation of the problem

Suppose that C_0^1 function $f(\mathbf{x})$, $\mathbf{x} \in \mathbb{R}^n$, $n \geqslant 2$ is compactly supported within the closed ball B of radius R centred at the origin. We will denote the boundary of the ball by ∂B. Our goal is to reconstruct $f(\mathbf{x})$ from its projections $g(\mathbf{z}, r)$ defined as the integrals of $f(\mathbf{x})$ over the spheres of radius r centred at $\mathbf{z}$:

$$g(\mathbf{z}, r) = \int_{\mathbb{S}^{n-1}} f(\mathbf{z} + r\hat{t}) r^{n-1} \, \mathrm{d}s(\hat{t}),$$

where $\mathbb{S}^{n-1}$ is the unit sphere in $\mathbb{R}^n$, $\hat{t}$ is a unit vector and $\mathrm{d}s$ is the normalized measure in $\mathbb{R}^n$. Projections are assumed to be known for all $\mathbf{z} \in \partial B$, $0 \leqslant r \leqslant 2R$ (integrals for $r > 2R$ automatically equal zero, since the corresponding integration spheres do not intersect the support of the function). In the following two sections we will present an explicit formula of backprojection type that solves this reconstruction problem.

2. Derivation

Our derivation is based on certain properties of the solutions of the Helmholtz equation in $\mathbb{R}^n$

$$\Delta h(\mathbf{x}) + \lambda^2 h(\mathbf{x}) = 0.$$

For this equation the free space Green's function $\Phi(\mathbf{x}, \mathbf{y}, \lambda)$ satisfying radiation boundary condition is described (see, for example [1]) by the formula

$$\Phi(\mathbf{x}, \mathbf{y}, \lambda) = \frac{\mathrm{i}}{4} \left(\frac{\lambda}{2\pi |\mathbf{x} - \mathbf{y}|} \right)^{n/2-1} H^{(1)}_{n/2-1}(\lambda |\mathbf{x} - \mathbf{y}|),$$

where $H^{(1)}_{n/2-1}(t)$ is the Hankel function of the first kind and of order $n/2 - 1$. To simplify the notation, we introduce functions $J(t)$, $N(t)$ and $H(t)$, defined by the following formulae:

$$J(t) = \frac{J_{n/2-1}(t)}{t^{n/2-1}}, \qquad N(t) = \frac{N_{n/2-1}(t)}{t^{n/2-1}}, \qquad H(t) = \frac{H^{(1)}_{n/2-1}(t)}{t^{n/2-1}} = J(t) + \mathrm{i}N(t),$$

where $J_{n/2-1}(t)$ and $N_{n/2-1}(t)$ are respectively the Bessel and Neumann functions of order $n/2 - 1$. In this notation Green's function $\Phi(\mathbf{x}, \mathbf{y}, \lambda)$ can be re-written in a simpler form:

$$\begin{aligned} \Phi(\mathbf{x}, \mathbf{y}, \lambda) &= \mathrm{i}c(\lambda, n) H(\lambda |\mathbf{x} - \mathbf{y}|) \\ &= c(\lambda, n)[\mathrm{i}J(\lambda |\mathbf{x} - \mathbf{y}|) - N(\lambda |\mathbf{x} - \mathbf{y}|)], \end{aligned}$$

where $c(\lambda, n)$ is a constant for a fixed value of λ:

$$c(\lambda, n) = \frac{\lambda^{n-2}}{4(2\pi)^{n/2-1}}.$$

We note that function $J(\lambda|\mathbf{x}|)$ is a solution of the Helmholtz equation for all $\mathbf{x} \in \mathbb{R}^n$, while $N(\lambda|\mathbf{x}|)$ solves this equation in $\mathbb{R}^n \backslash \{0\}$.

In order to derive the inversion formula, we utilize the following integral representation of f in the form of a convolution with $J(\lambda|\mathbf{y}-\mathbf{x}|)$:

$$f(\mathbf{y}) = \frac{1}{(2\pi)^{n/2}} \int_{\mathbb{R}^+} \left(\int_{\mathbb{R}^n} f(\mathbf{x}) J(\lambda|\mathbf{y}-\mathbf{x}|)\, \mathrm{d}x \right) \lambda^{n-1}\, \mathrm{d}\lambda. \tag{1}$$

The above equation easily follows from the Fourier representation of f

$$\begin{aligned} f(0) &= \frac{1}{(2\pi)^n} \int_{\mathbb{R}^n} \int_{\mathbb{R}^n} \mathrm{e}^{-\mathrm{i}\mathbf{x}\cdot\xi} f(\mathbf{x})\, \mathrm{d}\mathbf{x}\, \mathrm{d}\xi \\ &= \frac{1}{(2\pi)^n} \int_{\mathbb{R}^+} \int_{\mathbb{R}^n} f(\mathbf{x}) \left[\int_{\mathbb{S}^{n-1}} \mathrm{e}^{-\mathrm{i}\lambda\mathbf{x}\cdot\hat{\xi}}\, \mathrm{d}\hat{\xi} \right] \mathrm{d}\mathbf{x} \lambda^{n-1} \mathrm{d}\lambda \end{aligned}$$

and from the well-known integral representation for $J(|\mathbf{u}|)$ [17]

$$J(|\mathbf{u}|) = \frac{1}{(2\pi)^{n/2}} \int_{\mathbb{S}^{n-1}} \mathrm{e}^{\mathrm{i}\mathbf{u}\cdot\hat{\xi}}\, \mathrm{d}\hat{\xi}.$$

Let us denote the inner integral in (1) by $G_J(\mathbf{y}, \lambda)$

$$G_J(\mathbf{y}, \lambda) = \int_{\mathbb{R}^n} f(\mathbf{x}) J(\lambda|\mathbf{y}-\mathbf{x}|)\, \mathrm{d}x. \tag{2}$$

Similarly to the kernel $J(\lambda|\mathbf{y}-\mathbf{x}|)$ of this convolution, function $G_J(\mathbf{y}, \lambda)$ is an entire solution of the Helmholtz equation. Boundary values of this function $G_J(\mathbf{z}, \lambda), \mathbf{z} \in \partial B$ are easily computable from projections:

$$G_J(\mathbf{z}, \lambda) = \int_B f(\mathbf{x}) J_0(\lambda|\mathbf{z}-\mathbf{x}|)\, \mathrm{d}\mathbf{x} = \int_0^{2R} J_0(\lambda r) g(\mathbf{z}, r)\, \mathrm{d}r.$$

If λ is not in the spectrum of the Dirichlet Laplacian on B, $G_J(\mathbf{y}, \lambda)$ is completely determined by its boundary values and can be found by solving numerically the corresponding Dirichlet problem for the Helmholtz equation. Then $f(\mathbf{x})$ can be reconstructed from equation (1). Unfortunately, such a solution would not have an explicit form.

In order to obtain an explicit formula for $G_J(\mathbf{y}, \lambda)$ we will utilize a Helmholtz representation for $J(\lambda|\mathbf{y}-\mathbf{x}|)$; it results from an application of Green's formula and has the following form:

$$J(\lambda|\mathbf{y}-\mathbf{x}|) = \int_{\partial B} \left[J(\lambda|\mathbf{z}-\mathbf{x}| \frac{\partial}{\partial \mathbf{n}_\mathbf{z}} \Phi(\mathbf{y}, \mathbf{z}, \lambda) - \Phi(\mathbf{y}, \mathbf{z}, \lambda) \frac{\partial}{\partial \mathbf{n}_\mathbf{z}} J(\lambda|\mathbf{z}-\mathbf{x}|) \right] \mathrm{d}s(\mathbf{z}),$$

or

$$\begin{aligned} J(\lambda|\mathbf{y}-\mathbf{x}|) = -c(\lambda, n) \int_{\partial B} \Bigg[& J(\lambda|\mathbf{z}-\mathbf{x}| \frac{\partial}{\partial \mathbf{n}_\mathbf{z}} N(\lambda|\mathbf{y}-\mathbf{z}|) \\ & - N(\lambda|\mathbf{y}-\mathbf{z}|) \frac{\partial}{\partial \mathbf{n}_\mathbf{z}} J(\lambda|\mathbf{z}-\mathbf{x}|) \Bigg] \mathrm{d}s(\mathbf{z}). \end{aligned} \tag{3}$$

Such a representation is valid for any bounded connected domain with sufficiently regular boundary. A straightforward substitution of equation (3) into (2) leads to a boundary value representation for $G_J(\mathbf{y}, \lambda)$ involving the normal derivative of the latter function. Unlike the boundary values of $G_J(\mathbf{z}, \lambda)$, the normal derivative $\frac{\partial}{\partial \mathbf{n}_\mathbf{z}} G_J(\mathbf{z}, \lambda)$ cannot be explicitly computed from projections $g(\mathbf{z}, r)$.

This difficulty can be circumvented by modifying the Helmholtz representation as described below. We note that in the special case of a spherical domain the second integral in formula (3)

$$I(\mathbf{x}, \mathbf{y}) = \int_{\partial B} N(\lambda|\mathbf{y}-\mathbf{z}|) \frac{\partial}{\partial \mathbf{n}_\mathbf{z}} J(\lambda|\mathbf{z}-\mathbf{x}|)\, \mathrm{d}s(\mathbf{z}) \tag{4}$$

is a symmetric function of its arguments i.e. that

$$I(\mathbf{x}, \mathbf{y}) = I(\mathbf{y}, \mathbf{x}).$$

The proof of this fact is presented in the appendix. Using this symmetry we obtain a modified Helmholtz representation for $J(\lambda|\mathbf{y}-\mathbf{x}|)$:

$$J(\lambda|\mathbf{y}-\mathbf{x}|) = -c(\lambda, n)\int_{\partial B}\left[J(\lambda|\mathbf{z}-\mathbf{x}|\frac{\partial}{\partial \mathbf{n}_\mathbf{z}}N(\lambda|\mathbf{y}-\mathbf{z}|)\right.$$
$$\left. - N(\lambda|\mathbf{z}-\mathbf{x}|)\frac{\partial}{\partial \mathbf{n}_\mathbf{z}}J(\lambda|\mathbf{y}-\mathbf{z}|)\right] \mathrm{d}s(\mathbf{z}). \tag{5}$$

Now the substitution of equation (5) into (2) yields

$$\int_B f(\mathbf{x})J(\lambda|\mathbf{y}-\mathbf{x}|)\,\mathrm{d}x = -c(\lambda, n)\int_{\partial B}\left[\left(\int_B f(\mathbf{x})J(\lambda|\mathbf{z}-\mathbf{x}|)\,\mathrm{d}x\right)\frac{\partial}{\partial \mathbf{n}_\mathbf{z}}N(\lambda|\mathbf{y}-\mathbf{z}|)\right.$$
$$\left. - \left(\int_B f(\mathbf{x})N(\lambda|\mathbf{z}-\mathbf{x}|)\,\mathrm{d}x\right)\frac{\partial}{\partial \mathbf{n}_\mathbf{z}}J(\lambda|\mathbf{y}-\mathbf{z}|)\right] \mathrm{d}s(\mathbf{z}),$$

where the inner integrals are easily computable from the projections $g(\mathbf{z}, t)$:

$$\int_B f(\mathbf{x})J(\lambda|\mathbf{z}-\mathbf{x}|)\,\mathrm{d}x = \int_0^{2R} J(\lambda t)g(\mathbf{z}, t)\,\mathrm{d}t,$$
$$\int_B f(\mathbf{x})N(\lambda|\mathbf{z}-\mathbf{x}|)\,\mathrm{d}x = \int_0^{2R} N(\lambda t)g(\mathbf{z}, t)\,\mathrm{d}t.$$

Thus, the convolution of f and J can be reconstructed from the projections as follows:

$$\int_B f(\mathbf{x})J(\lambda|\mathbf{y}-\mathbf{x}|)\,\mathrm{d}x = -c(\lambda, n)\int_{\partial B}\left[\left(\int_0^{2R} J(\lambda t)g(\mathbf{z}, t)\,\mathrm{d}t\right)\frac{\partial}{\partial \mathbf{n}_\mathbf{z}}N(\lambda|\mathbf{y}-\mathbf{z}|)\right.$$
$$\left. - \left(\int_0^{2R} N(\lambda t)g(\mathbf{z}, t)\,\mathrm{d}t\right)\frac{\partial}{\partial \mathbf{n}_\mathbf{z}}J(\lambda|\mathbf{y}-\mathbf{z}|)\right] \mathrm{d}s(\mathbf{z})$$
$$= c(\lambda, n)\mathrm{div}\int_{\partial B}\mathbf{n}(\mathbf{z})\left[\left(\int_0^{2R} J(\lambda t)g(\mathbf{z}, t)\,\mathrm{d}t\right)N(\lambda|\mathbf{y}-\mathbf{z}|)\right.$$
$$\left. - \left(\int_0^{2R} N(\lambda t)g(\mathbf{z}, t)\,\mathrm{d}t\right)J(\lambda|\mathbf{y}-\mathbf{z}|)\right] \mathrm{d}s(\mathbf{z}). \tag{6}$$

Finally, by combining equations (1) and (6), one arrives at the following inversion formula:

$$f(\mathbf{y}) = \frac{1}{4(2\pi)^{n-1}}\mathrm{div}\int_{\partial B}\mathbf{n}(\mathbf{z})h(\mathbf{z}, |\mathbf{y}-\mathbf{z}|)\,\mathrm{d}s(\mathbf{z}),$$

where

$$h(\mathbf{z}, t) = \int_{\mathbb{R}^+}\left[N(\lambda t)\left(\int_0^{2R} J(\lambda t')g(\mathbf{z}, t')\,\mathrm{d}t'\right) - J(\lambda t)\left(\int_0^{2R} N(\lambda t')g(\mathbf{z}, t')\,\mathrm{d}t'\right)\right]\lambda^{2n-3}\,\mathrm{d}\lambda.$$

3. Particular cases

3.1. 2D case

From the point of view of practical applications the two- and three-dimensional cases are the most important ones. In 2D, $J(t) = J_0(t)$, $N(t) = N_0(t)$ and the inversion formula has the following form:

$$f(\mathbf{y}) = \frac{1}{8\pi}\mathrm{div}\int_{\partial B}\mathbf{n}(\mathbf{z})h(\mathbf{z}, |\mathbf{y}-\mathbf{z}|)\,\mathrm{d}l(\mathbf{z}), \tag{7}$$

where

$$h(\mathbf{z},t)=\int_{\mathbb{R}^+}\left[N_0(\lambda t)\left(\int_0^{2R}J_0(\lambda t')g(\mathbf{z},t')\,\mathrm{d}t'\right)-J_0(\lambda t)\left(\int_0^{2R}N_0(\lambda t')g(\mathbf{z},t')\,\mathrm{d}t'\right)\right]\lambda\,\mathrm{d}\lambda. \tag{8}$$

Equation (7) is a backprojection followed by the divergence operator. It is worth noting that such a divergence form of a reconstruction formula is not unusual; it also naturally occurs in reconstruction formulae for the attenuated Radon transform (see, for instance [20]).

Equation (8) represents the filtration step of the algorithm. In order to better understand the nature of this operator we re-write (8) in the form

$$\begin{aligned}h(\mathbf{z},t)=-\frac{\mathrm{i}}{2}\int_{\mathbb{R}^+}&\left[H_0^{(1)}(\lambda t)\left(\int_0^{2R}\overline{H_0^{(1)}(\lambda t')}g(\mathbf{z},t')\,\mathrm{d}t'\right)\right.\\&\left.-\overline{H_0^{(1)}(\lambda t)}\left(\int_0^{2R}H_0^{(1)}(\lambda t')g(\mathbf{z},t')\,\mathrm{d}t'\right)\right]\lambda\,\mathrm{d}\lambda\end{aligned} \tag{9}$$

and recall that for large values of the argument t the Hankel function $H_0^{(1)}(t)$ has the following asymptotic expansion ([19]):

$$H_0^{(1)}(t)=\left(\frac{2}{\pi t}\right)^{\frac{1}{2}}\mathrm{e}^{-\frac{\mathrm{i}}{2}\pi}\,\mathrm{e}^{\mathrm{i}t}.$$

In the situation when the support of the function $f(\mathbf{x})$ remains bounded and the radius R of the ball B becomes large, the inner and outer integrals in (9) reduce to the direct and inverse Fourier transforms, with one of the terms corresponding to the positive frequencies and the other to the negative ones. Thus, since the two terms have opposite signs, in the asymptotic limit of large R operator (9) equals (up to a constant factor) to the Hilbert transform of $g(\mathbf{z},\cdot)$.

3.2. 3D case

In the three-dimensional case

$$J(t)=\frac{J_{1/2}(\lambda r)}{\sqrt{\lambda r}}=\sqrt{\frac{2}{\pi}}j_0(\lambda r),\qquad N(t)=\frac{N_{1/2}(\lambda r)}{\sqrt{\lambda r}}=\sqrt{\frac{2}{\pi}}n_0(\lambda r),$$

where $j_0(t)$ and $n_0(t)$ are the spherical Bessel and Neumann functions respectively. The formula takes the following form:

$$f(\mathbf{y})=\frac{1}{16\pi^2}\mathrm{div}\int_{|z|=R}\mathbf{n}(\mathbf{z})h(\mathbf{z},|\mathbf{y}-\mathbf{z}|)\,\mathrm{d}s(\mathbf{z}), \tag{10}$$

with

$$\begin{aligned}h(\mathbf{z},t)=\frac{2}{\pi}\int_{\mathbb{R}^+}&\left[n_0(\lambda t)\left(\int_0^{2R}j_0(\lambda t')g(\mathbf{z},t')\,\mathrm{d}t'\right)\right.\\&\left.-j_0(\lambda t)\left(\int_0^{2R}n_0(\lambda t')g(\mathbf{z},t')\,\mathrm{d}t'\right)\right]\lambda^3\,\mathrm{d}\lambda.\end{aligned}$$

In this case, however, a further simplification is possible since $j_0(t)$ and $n_0(t)$ have a simple representation in terms of trigonometric functions:

$$j_0(t)=\frac{\sin t}{t},\qquad n_0(t)=-\frac{\cos t}{t}.$$

The substitution of these trigonometric expressions into the inversion formula leads to a significantly simpler formula:

$$\begin{aligned} h(\mathbf{z},t) &= -\frac{2}{\pi t}\int_{\mathbb{R}^+}\cos(\lambda t)\left[\int_0^{2R}\sin(\lambda t')\frac{g(\mathbf{z},t')}{t'}\,\mathrm{d}t'\right]\lambda\,\mathrm{d}\lambda \\ &\quad + \frac{2}{\pi t}\int_{\mathbb{R}^+}\sin(\lambda t)\left[\int_0^{2R}\cos(\lambda t')\frac{g(\mathbf{z},t')}{t'}\,\mathrm{d}t'\right]\lambda\,\mathrm{d}\lambda \\ &= -\frac{2}{\pi t}\frac{\mathrm{d}}{\mathrm{d}t}\int_{\mathbb{R}^+}\sin(\lambda t)\left[\int_0^{2R}\sin(\lambda t')\frac{g(\mathbf{z},t')}{t'}\,\mathrm{d}t'\right]\mathrm{d}\lambda \\ &\quad - \frac{2}{\pi t}\frac{\mathrm{d}}{\mathrm{d}t}\int_{\mathbb{R}^+}\cos(\lambda t)\left[\int_0^{2R}\cos(\lambda t')\frac{g(\mathbf{z},t')}{t'}\,\mathrm{d}t'\right]\mathrm{d}\lambda \\ &= -\frac{2}{t}\frac{\mathrm{d}}{\mathrm{d}t}\frac{g(\mathbf{z},t)}{t}, \end{aligned} \tag{11}$$

where we took into account the fact that the Fourier sine and cosine transforms are self-invertible. By combining (11) and (10) our inversion formula can be re-written in the form

$$f(\mathbf{y}) = -\frac{1}{8\pi^2}\mathrm{div}\int_{\partial B}\mathbf{n}(\mathbf{z})\left(\frac{1}{t}\frac{\mathrm{d}}{\mathrm{d}t}\frac{g(\mathbf{z},t)}{t}\right)\Big|_{t=|\mathbf{z}-\mathbf{y}|}\mathrm{d}s(\mathbf{z}). \tag{12}$$

This expression is equivalent to one of the formulae derived in [22] for the 3D case.

An inversion formula more convenient for numerical implementation can be derived from (12) by moving the divergence operator inside the integral and replacing the cosine in the expression for the normal derivative by $\frac{\mathbf{z}\cdot(\mathbf{y}-\mathbf{z})}{R|\mathbf{y}-\mathbf{z}|}$:

$$f(\mathbf{y}) = \frac{1}{8\pi^2}\int_{\partial B}\left(\frac{\mathrm{d}}{\mathrm{d}t}\left[\frac{1}{t}\frac{\mathrm{d}}{\mathrm{d}t}\frac{g(\mathbf{z},t)}{t}\right]\right)\Big|_{t=|\mathbf{y}-\mathbf{z}|}\frac{\mathbf{z}\cdot(\mathbf{y}-\mathbf{z})}{R|\mathbf{y}-\mathbf{z}|}\,\mathrm{d}s(\mathbf{z}). \tag{13}$$

4. Numerical implementation

4.1. 2D case

Our 2D algorithm results from the straightforward discretization of the reconstruction formulae (7), (8). The divergence operator in (7) is approximated by the standard second-order central differences

$$\frac{\partial}{\partial y_j}u(\mathbf{y}) \approx \frac{1}{2\Delta y}[u(\mathbf{y}+\Delta y\,\mathbf{e}_j) - u(\mathbf{y}-\Delta y\,\mathbf{e}_j)], \qquad j=1,2,$$

where Δy is the step of the computational grid, $\mathbf{e}_1 = (1,0)$, $\mathbf{e}_2 = (0,1)$.

Certain care should be taken when computing the oscillatory integrals in (8). Let us assume that measurements $g(\mathbf{z},t)$ made by the detector located at the point $\mathbf{z}$ are discretized in t with the discretization step $\Delta t = 2R/N$, where N is the number of taken samples. Then the range of frequencies λ that can be used in (8) is bounded by the Nyquist frequency $\lambda_N = \pi/\Delta t = \pi N/(2R)$. On the other hand, $g(\mathbf{z},t)$ is finitely supported (in t) within the symmetric interval $(-2R, 2R)$; thus the maximal (Nyquist) discretization step $\Delta\lambda_{\max}$ in the frequency domain equals $\pi/(2R)$. We choose to use $\Delta\lambda_{\max}$ as the discretization step in λ since, as our numerical experiments have shown, over-sampling does not noticeably improve the quality of the reconstructed image. Thus, when evaluating (8) we compute the integrals for the set of frequencies λ_k uniformly distributed over the interval $(0, \pi N/(2R))$ with the step $\pi/(2R)$; obviously there is N such values. All integrals in (8) are approximated by the trapezoidal rule.

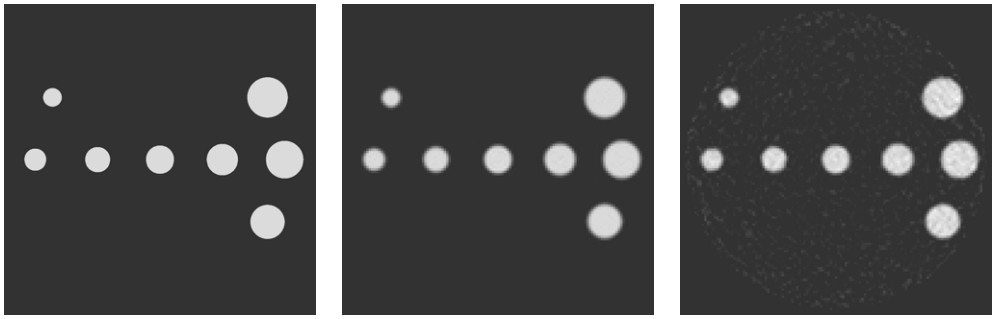

(a) (b) (c)

Figure 1. Reconstruction in 2D: (a) the phantom, (b) reconstruction from the exact data and (c) reconstruction from the noisy data.

In the experiments presented here we utilized the phantom shown in figure 1(a). This function, supported within the unit disk, is the sum of eight characteristic functions of disks with radii ranging from 0.06 to 0.13. The 129 × 129 images presented in figures 1(b) and (c) were reconstructed from 256 projections each containing 129 samples. The projections correspond to 256 detectors uniformly distributed over the circle of radius 1.1 centred at the origin. Figure 1(b) demonstrates the image reconstructed from the exact data, while figure 1(c) shows the result of the reconstruction from noisy data. In the latter case the measurement noise in the projections was modelled by adding to the exact data the values of a normally distributed random variable. The noise component was scaled so that its L_2 norm was equal to 15% of the norm of the signal. The reconstruction from the noisy data (figure 1(c)) demonstrates high stability of the algorithm to the noise. The image seems to be almost too good, given the high level of noise (15%) present in the projections. In part, this is a result of the high-contrast phantom we used; a lower contrast image would be affected by the noise to a larger extent.

4.2. 3D case

Our 3D algorithm is obtained by discretizing formula (13). We approximate both 1D derivatives in this formula by the fourth-order accurate central differences

$$u'(t) \approx \frac{1}{12\Delta t}[8(u(t+\Delta t) - u(t-\Delta t)) - (u(t+2\Delta t) - u(t-2\Delta t))].$$

Use of such higher order finite differences helps us to avoid inordinate smoothing of edges in the image.

The phantom we used for the numerical experiments in 3D is somewhat similar to the one used in the previous section. It is defined as the sum of eight characteristic functions of the balls with radii ranging from 0.06 to 0.13, whose centres lie in the plane $x_3 = 0$. The cross section of the phantom by the latter plane is shown in figure 2(a); incidentally, it coincides with the image shown in figure 1(a). The model projections were computed for the detectors lying on the sphere of radius 1.1 centred at the origin; detectors were placed at the nodes of the product grid, uniform in θ and Gaussian in $s = \cos\varphi$, where θ and φ are the standard spherical coordinates. The detector grid was of dimension 256×129 respectively in θ and φ. The discretization in t was uniform with 129 nodes, i.e. each projection consisted of 129 values of spherical integrals.

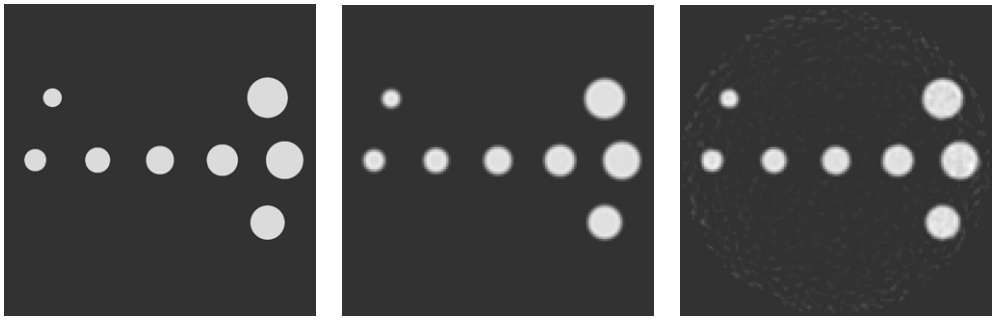

(a) (b) (c)

Figure 2. 3D reconstruction, section by the plane $x_3 = 0$: (a) the phantom, (b) reconstruction from the exact data and (c) reconstruction from the noisy data.

The images were reconstructed on $129 \times 129 \times 129$ Cartesin grid. Figure 2(b) shows the central cross section ($x_3 = 0$) of the reconstruction from the exact data. As in the previous section, imprecise measurements were modelled by an additive normally distributed noise with intensity 15% of the signal (in L_2-norm). The result of the reconstruction from the noisy data is presented in figure 2(c); again, it demonstrates high stability of the algorithm to the perturbations of the data.

Acknowledgments

The author would like to thank P Kuchment for fruitful discussions and numerous helpful comments. This work was partially supported by the NSF/DMS grant NSF-0312292 and by the DOE grant DE-FG02-03ER25577.

Appendix A

In this section we prove that for arbitrary $\mathbf{x}, \mathbf{y} \in B$ function $I(\mathbf{x}, \mathbf{y})$ defined by equation (4) is a symmetric function of its arguments, i.e. that $I(\mathbf{x}, \mathbf{y}) = I(\mathbf{y}, \mathbf{x})$.

First we need to find a closed-form expression for a single layer potential of a spherical shell with the density equal to a spherical harmonic $Y_l^{(k)}(\hat{x})$. To this end we introduce functions $u_\lambda^{k,l}(\mathbf{x})$ and $v_\lambda^{k,l}(\mathbf{x})$ defined as follows:

$$u_\lambda^{k,l}(\mathbf{x}) = Y_l^{(k)}(\hat{x}) J_{(k)}(\lambda|\mathbf{x}|),$$
$$v_\lambda^{k,l}(\mathbf{x}) = Y_l^{(k)}(\hat{x}) H_{(k)}(\lambda|\mathbf{x}|), \qquad \hat{x} = \mathbf{x}/|\mathbf{x}|,$$

where we, as before, utilize the notation

$$J_{(k)}(t) = \frac{J_{n/2+k-1}(t)}{t^{n/2-1}},$$
$$N_{(k)}(t) = \frac{N_{n/2+k-1}(t)}{t^{n/2-1}},$$
$$H_{(k)}(t) = \frac{H^{(1)}_{n/2+k-1}(t)}{t^{n/2-1}}.$$

Functions $u_\lambda^{k,l}(\mathbf{x})$ are ([18]) entire solutions of the Helmholtz equation for all $\mathbf{x} \in \mathbb{R}^n$, while $v_\lambda^{k,l}(\mathbf{x})$ are radiating solutions of this equation in $\mathbb{R}^n \backslash \{0\}$. If we apply the Green's theorem in

an exterior of a sphere of radius r_0 to functions $u_\lambda^{k,l}(\mathbf{x})$ and $v_\lambda^{k,l}(\mathbf{x})$, we will obtain (for $|\mathbf{x}| > r_0$)

$$\begin{aligned} 0 &= \int_{|\mathbf{z}|=r_0} \left[u_\lambda^{k,l}(\mathbf{z}) \frac{\partial}{\partial \mathbf{n}_\mathbf{z}} \Phi(\mathbf{x}, \mathbf{z}, \lambda) - \Phi(\mathbf{x}, \mathbf{z}, \lambda) \frac{\partial}{\partial \mathbf{n}_\mathbf{z}} u_\lambda^{k,l}(\mathbf{z}) \right] \mathrm{d}\mathbf{z} \\ &= \int_{|\mathbf{z}|=r_0} Y_l^{(k)}(\hat{z}) \left[J_{(k)}(\lambda r_0) \frac{\partial}{\partial \mathbf{n}_\mathbf{z}} \Phi(\mathbf{x}, \mathbf{z}, \lambda) - \Phi(\mathbf{x}, \mathbf{z}, \lambda) \lambda J'_{(k)}(\lambda r_0) \right] \mathrm{d}\mathbf{z}, \end{aligned}$$

and

$$\begin{aligned} v_\lambda^{k,l}(\mathbf{x}) &= \int_{|\mathbf{z}|=r_0} \left[v_\lambda^{k,l}(\mathbf{z}) \frac{\partial}{\partial \mathbf{n}_\mathbf{z}} \Phi(\mathbf{x}, \mathbf{z}, \lambda) - \Phi(\mathbf{x}, \mathbf{z}, \lambda) \frac{\partial}{\partial \mathbf{n}_\mathbf{z}} v_\lambda^{k,l}(\mathbf{z}) \right] \mathrm{d}\mathbf{z} \\ &= \int_{|\mathbf{z}|=r_0} Y_l^{(k)}(\hat{z}) \left[H_{(k)}(\lambda r_0) \frac{\partial}{\partial \mathbf{n}_\mathbf{z}} \Phi(\mathbf{x}, \mathbf{z}, \lambda) - \Phi(\mathbf{x}, \mathbf{z}, \lambda) \lambda H'_{(k)}(\lambda r_0) \right] \mathrm{d}\mathbf{z}, \end{aligned}$$

where $\hat{z} = \mathbf{z}/|\mathbf{z}|$. By combining the above two equations one can eliminate the terms with $\frac{\partial}{\partial \mathbf{n}_\mathbf{z}}$:

$$J_{(k)}(\lambda r_0) v_\lambda^{k,l}(\mathbf{x}) = \lambda [H_{(k)}(\lambda r_0) J'_{(k)}(\lambda r_0) - J_{(k)}(\lambda r_0) H'_{(k)}(\lambda r_0)] \int_{|\mathbf{z}|=r_0} Y_l^{(k)}(\hat{z}) \Phi(\mathbf{x}, \mathbf{z}, \lambda) \, \mathrm{d}\mathbf{z}. \tag{A.1}$$

The expression in the brackets can be simplified using the well-known formula [19] for the Wronskian of $H_\alpha^{(0)}(t)$ and $J_\alpha(t)$:

$$H_\alpha^{(0)}(t) J'_\alpha(t) - J_\alpha(t) (H_\alpha^{(0)})'(t) = -\frac{\mathrm{i}}{2\pi t}.$$

Formula (A.1) then takes form

$$J_{(k)}(\lambda r_0) v_\lambda^{k,l}(\mathbf{x}) = -\frac{\mathrm{i}}{2\pi r_0 (\lambda r_0)^{n-2}} \int_{|\mathbf{z}|=r_0} Y_l^{(k)}(\hat{z}) \Phi(\mathbf{x}, \mathbf{z}, \lambda) \, \mathrm{d}\mathbf{z}$$

so that the single layer potential we consider is described by the following equation:

$$\int_{|\mathbf{z}|=r_0} Y_l^{(k)}(\hat{z}) \Phi(\mathbf{x}, \mathbf{z}, \lambda) \, \mathrm{d}\mathbf{z} = \mathrm{i} 2\pi r_0 (\lambda r_0)^{n-2} J_{(k)}(\lambda r_0) H_{(k)}(\lambda |\mathbf{x}|) Y_l^{(k)}(\hat{x}). \tag{A.2}$$

By substituting into (A.2) the expression for the Green's function $\Phi(\mathbf{x}, \mathbf{z}, \lambda)$ in the form

$$\Phi(\mathbf{x}, \mathbf{z}, \lambda) = \mathrm{i} c(\lambda, n) H(\lambda |\mathbf{x} - \mathbf{z}|)$$

one obtains

$$\int_{|\mathbf{z}|=r_0} Y_l^{(k)}(\hat{z}) H(\lambda |\mathbf{x} - \mathbf{z}|) \, \mathrm{d}\mathbf{z} = \frac{2\pi r_0 (\lambda r_0)^{n-2}}{c(\lambda, n)} J_{(k)}(\lambda r_0) H_{(k)}(\lambda |\mathbf{x}|) Y_l^{(k)}(\hat{x}).$$

Finally, by separating the real and imaginary parts of the above equation we arrive at the following two formulae:

$$\int_{|\mathbf{z}|=r_0} Y_l^{(k)}(\hat{z}) J(\lambda |\mathbf{x} - \mathbf{z}|) \, \mathrm{d}\mathbf{z} = \frac{2\pi r_0 (\lambda r_0)^{n-2}}{c(\lambda, n)} J_{(k)}(\lambda r_0) J_{(k)}(\lambda |\mathbf{x}|) Y_l^{(k)}(\hat{x}), \tag{A.3}$$

$$\int_{|\mathbf{z}|=r_0} Y_l^{(k)}(\hat{z}) N(\lambda |\mathbf{x} - \mathbf{z}|) \, \mathrm{d}\mathbf{z} = \frac{2\pi r_0 (\lambda r_0)^{n-2}}{c(\lambda, n)} J_{(k)}(\lambda r_0) N_{(k)}(\lambda |\mathbf{x}|) Y_l^{(k)}(\hat{x}), \tag{A.4}$$

valid for $|\mathbf{x}| > r_0$. This completes the preparation for the proof of the symmetry of $I(\mathbf{x}, \mathbf{y})$.

Let us consider function $I(\alpha \hat{x}, \beta \hat{y})$. For fixed values of α and β this is an infinitely smooth function of $\hat{x}$ and $\hat{y}$ defined on $\mathbb{S}^{n-1} \times \mathbb{S}^{n-1}$. Consider the Fourier expansion of $I(\alpha \hat{x}, \beta \hat{y})$ in

the spherical harmonics in both variables $\hat{x}$ and $\hat{y}$. Coefficients of such series are given by the formula

$$a^{k,l}_{k',l'}(\alpha,\beta)=\int_{\mathbb{S}^{n-1}}\int_{\mathbb{S}^{n-1}} Y^k_l(\hat{x})Y^{k'}_{l'}(\hat{y})I(\alpha\hat{x},\beta\hat{y})\,\mathrm{d}\hat{x}\,\mathrm{d}\hat{y} \tag{A.5}$$

with $k=0,1,2,\ldots,0\leqslant l\leqslant d_k$,

$$d_0=1,\qquad d_1=n,$$
$$d_k=\binom{n+k-1}{k}-\binom{n+k-3}{k-2},\qquad k\geqslant 2.$$

In order to prove the symmetry $I(\mathbf{x},\mathbf{y})=I(\mathbf{y},\mathbf{x})$ it is enough to prove that

$$a^{k,l}_{k',l'}(\alpha,\beta)=a^{k',l'}_{k,l}(\beta,\alpha) \tag{A.6}$$

for all relevant values of k,k',l,l'. By substituting the expression for $I(\alpha\hat{x},\beta\hat{y})$ into (A.5) one obtains

$$\begin{aligned}
a^{k,l}_{k',l'}(\alpha,\beta)&=\int_{\mathbb{S}^{n-1}}\int_{\mathbb{S}^{n-1}} Y^k_l(\hat{x})Y^{k'}_{l'}(\hat{y})\left[\int_{|\mathbf{z}|=R} N(\lambda|\mathbf{z}-\alpha\hat{x}|)\frac{\partial}{\partial\mathbf{n}_\mathbf{z}}J(\beta\hat{y}-\mathbf{z}|)\mathrm{d}\mathbf{z}\right]\mathrm{d}\hat{x}\,\mathrm{d}\hat{y}\\
&=\int_{\mathbb{S}^{n-1}} Y^{k'}_{l'}(\hat{y})\left[\int_{|\mathbf{z}|=R}\left(\int_{\mathbb{S}^{n-1}} Y^k_l(\hat{x})N(\lambda|\mathbf{z}-\alpha\hat{x}|)\,\mathrm{d}\hat{x}\right)\frac{\partial}{\partial\mathbf{n}_\mathbf{z}}J(\lambda|\beta\hat{y}-\mathbf{z}|\,\mathrm{d}\mathbf{z}\right]\mathrm{d}\hat{y}\\
&=\frac{1}{\alpha^{n-1}}\int_{\mathbb{S}^{n-1}} Y^{k'}_{l'}(\hat{y})\left[\int_{|\mathbf{z}|=R}\left(\int_{|u|=|\mathbf{x}|} Y^k_l(u/|u|)N(\lambda|\mathbf{z}-u|)\mathrm{d}u\right)\right.\\
&\left.\times\frac{\partial}{\partial\mathbf{n}_\mathbf{z}}J(\lambda|\beta\hat{y}-\mathbf{z}|\,\mathrm{d}\mathbf{z}\right]\mathrm{d}\hat{y}.
\end{aligned}$$

Utilizing formulae (A.3), (A.4) and the orthonormality of the spherical harmonics we find that $a^{k,l}_{k',l'}(\alpha,\beta)=0$ if $k\neq k'$ or $l\neq l'$. Otherwise

$$a^{k,l}_{k,l}(\alpha,\beta)=\lambda\left(\frac{2\pi\lambda^{n-2}}{c(\lambda,n)}\right)^2 R^{n-1}J_{(k)}(\lambda\alpha)J_{(k)}(\lambda\beta)N_{(k)}(\lambda R)J'_{(k)}(\lambda R).$$

Inspection of the above formula shows that coefficients $a^{k,l}_{k',l'}(\alpha,\beta)$ indeed satisfy (A.6) and, thus, that $I(\mathbf{x},\mathbf{y})=I(\mathbf{y},\mathbf{x})$.

References

[1] Agmon S 1990 A representation theorem for solutions of the Helmholtz equation and resolvent estimates for the Laplacian *Analysis, et cetera* ed P Rabinowitz and E Zehnder (Boston: Academic) pp 39–76

[2] Agranovsky M, Kuchment P and Quinto E T 2006 Range descriptions for the spherical mean Radon transform *Preprint* math.AP/0606314

[3] Agranovsky M L and Quinto E T 1996 Injectivity sets for the Radon transform over circles and complete systems of radial functions *J. Funct. Anal.* **139** 383–414

[4] Ambartsoumian G and Kuchment P 2005 On the injectivity of the circular Radon transform arising in thermoacoustic tomography *Inverse Problems* **21** 473–85

[5] Ambartsoumian G and Kuchment P 2006 A range description for the planar circular Radon transform *SIAM J. Math. Anal.* **38** 681–92

[6] Ambartsoumian G and Patch S K 2005 Thermoacoustic tomography—implementation of exact backprojection formulae *Preprint* math.NA/0510638

[7] Bérard P 1979 Spectres et Groupes Cristallographiques *C. R. Acad. Sci. Paris A-B* **288** A1059–60

[8] Bérard P and Besson G 1980 Spectres et Groupes Cristallographiques II: Domaines Sphériques *Ann. Inst. Fourier* **30** 237–48

[9] Finch D, Rakesh and Patch S 2004 Determining a function from its mean values over a family of spheres *SIAM J. Math. Anal.* **35** 1213–40

[10] Finch D and Rakesh 2006 The range of the spherical mean value operator for functions supported in a ball *Inverse Problems* **22** 923–38
[11] Finch D, Haltmeier M and Rakesh 2006 Inversion of spherical means and the wave equation in even dimensions *Preprint*
[12] Kruger R A, Liu P, Fang Y R and Appledorn C R 1995 Photoacoustic ultrasound (PAUS) reconstruction tomography *Med. Phys.* **22** 1605–9
[13] Kruger R A, Reinecke D R and Kruger G A 1999 GA Thermoacoustic computed tomography—technical considerations *Med. Phys.* **26** 1832–7
[14] Kuchment P 2006 Generalized transforms of radon type and their applications *The Radon Transform, Inverse Problems, and Tomography (Proc. Symp. Appl. Math.* vol 63*)* ed G Olafsson and E T Quinto (Providence, RI: American Mathematical Society) pp 67–91
[15] Norton S J 1980 Reconstruction of a two-dimensional reflecting medium over a circular domain: exact solution *J. Acoust. Soc. Am.* **67** 1266–73
[16] Norton S J and Linzer M 1981 Ultrasonic reflectivity imaging in three dimensions—exact inverse scattering solutions for plane, cylindrical, and spherical apertures *IEEE Trans. Biomed. Eng.* **28** 202–20
[17] Stein E M and Weiss G 1971 *Introduction to Fourier Analysis on Euclidean Spaces* (Princeton, NJ: Princeton University Press)
[18] Volchkov V V 2003 *Integral Geometry and Convolution Equations* (Dordrecht: Kluwer)
[19] Watson G N 1922 *A Treatise on the Theory of Bessel Functions* (Cambridge: Cambridge University Press)
[20] Novikov R G 2002 An inversion formula for the attenuated x-ray transformation *Ark. Mat.* **40** 145–67
[21] M. Xu and Wang L-H V 2002 Time-domain reconstruction for thermoacoustic tomography in a spherical geometry *IEEE Trans. Med. Imaging* **21** 814–22
[22] Xu M and Wang L V 2005 Universal back-projection algorithm for photoacoustic computed tomography *Phys. Rev.* E **71** 016706